Suga, N., and W. E. O'Neill (1980) Auditory processing of echoes: Representation of acoustic information from the environment in the bat cerebral cortex. In *Animal Sonar Systems*, R. G. Busnel and J. F. Fish, eds., pp. 589–611, Plenum, New York.

Suga, N., and K. Tsuzuki (1985) Inhibition and level-tolerant frequency tuning in the auditory cortex of the mustached bat. *J. Neurophysiol.* 53:1109–1145.

Suga, N., and Y. Yajima (1988) Audio-visual integration in the midbrain of the mustached bat: Periaqueductal gray and reticular formation. In *The Physiological Control of Mammalian Vocalization*, J. D. Newman, ed., Plenum, New York (in press).

Suga, N., J. A. Simmons, and T. Shimozawa (1974) Neurophysiological studies on echolocation systems in awake bats producing CF-FM orientation sounds. *J. Exp. Biol.* 61:379–399.

Suga, N., J. A. Simmons, and P. H.-S. Jen (1975) Peripheral specialization for fine analysis of Doppler-shifted echoes in "CF-FM" bat *Pteronotus parnellii*. *J. Exp. Biol.* 63:161–192.

Suga, N., G. Neuweiler, and J. Möller (1976) Peripheral auditory tuning for fine frequency analysis by the CF-FM bat, *Rhinolophus ferrumequinum*. IV. Properties of peripheral auditory neurons. *J. Comp. Physiol.* 106:111–125.

Suga, N., W. E. O'Neill, and T. Manabe (1978) Cortical neurons sensitive to particular combinations of information bearing elements of bio-sonar signals in the mustached bat. *Science* 200:778–781.

Suga, N., W. E. O'Neill, and T. Manabe (1979) Harmonic-sensitive neurons in the auditory cortex of the mustached bat. *Science* 203:270–274.

Suga, N., K. Kujirai, and W. E. O'Neill (1981) How biosonar information is represented in the bat cerebral cortex. In *Neuronal Mechanisms of Hearing*, J. Syka and L. Aitkin, eds., pp. 197–219, Plenum, New York.

Suga, N., W. E. O'Neill, K. Kujirai, and T. Manabe (1983a) Specialization of "combination-sensitive" neurons for processing of complex biosonar signals in the auditory cortex of the mustached bat. *J. Neurophysiol.* 49:1573–1626.

Suga, N., H. Niwa, and I. Taniguchi (1983b) Representation of biosonar information in the auditory cortex of the mustached bat, with emphasis on representation of target velocity information. In *Advances in Vertebrate Neuroethology*, P. Ewert, ed., pp. 829–867, Plenum, New York.

Suga, N., H. Niwa, I. Taniguchi, and D. Margoliash (1987) The personalized auditory cortex of the mustached bat: Adaptation for echolocation. *J. Neurophysiol.* 58:643–654.

Sullivan, W. E., III (1982a) Neural representation of target distance in auditory cortex of the echolocating bat *Myotis lucifigus*. *J. Neurophysiol.* 48:1011–1032.

Sullivan, W. E., III (1982b) Possible neural mechanisms of target distance coding in auditory system of the echolocating bat *Myotis lucifigus*. *J. Neurophysiol.* 48:1033–1047.

Sullivan, W. E., III, and M. Konishi (1984) Segregation of stimulus phase and intensity coding in the cochlear nucleus of the barn owl. *J. Neurosci.* 4:1787–1799.

Symmes, D. (1981) On the use of natural stimuli in neurophysiological studies of audition (review). *Hear. Res.* 4:203–214.

Tsuzuki, K., and N. Suga (1988) Combination-sensitive neurons in the ventrolateral area of the auditory cortex of the mustached bat. *J. Neurophysiol.* (submitted).

Tunturi, A. R. (1952) A difference in the representation of auditory signal for the left and right ears in the iso-frequency contours of the right middle ectosylvian and auditory cortex of the dog. *Am. J. Physiol.* 168:712–727.

Watanabe, T. (1959) A single neuron activity in the secondary cortical auditory area in the cat. *Jpn. J. Physiol.* 9:245–256.

Wever, E. G. (1949) *Theory of Hearing*, Wiley, New York.

Yin, T. C. T., and S. Kuwada (1984) Neural mechanisms of binaural interaction. In *Dynamic Aspects of Neocortical Function*, G. M. Edelman, W. E. Gall, and W. M. Cowan, eds., pp. 263–313, Wiley, New York.

Young, E. D., and M. B. Sachs (1979) Representation of steady-state vowels in the temporal aspects of the discharge patterns of populations of auditory nerve fibers. *J. Acoust. Soc. Am.* 66:1381–1403.

Chapter 24

Neurophysiological and Anatomical Substrates of Sound Localization in the Owl

MASAKAZU KONISHI
TERRY T. TAKAHASHI
HERMANN WAGNER
WINTHROP E. SULLIVAN
CATHERINE E. CARR

ABSTRACT

The ideas that guided the present work include the integration of behavioral, physiological, and anatomical approaches, the selection of an animal appropriate for the question to be addressed, the use of natural behavior and stimuli, and the study of successive stages of stimulus processing starting from higher-order complex neurons. The barn owl is particularly suitable for the study of sound localization because of its exquisite ability to track prey by hearing. The owl uses interaural time and intensity differences to localize sound in azimuth and elevation, respectively. The binaural time and intensity cues are processed in anatomically separate pathways that start from the cochlear nuclei.

The owl's auditory system measures interaural time difference in a noise signal by using the phase of its spectral components. The nucleus laminaris, the first site of binaural convergence in the time pathway, receives phase information in the form of phase-locked spikes from the nucleus magnocellularis. We hypothesize that the nucleus laminaris uses the principles of coincidence detection and delay lines to measure interaural time differences in different frequency bands. These mechanisms underlie the origin of neuronal selectivity for interaural time differences. When a neuron is selective for a particular time disparity independent of stimulus frequency, the neuron is said to have a characteristic delay. All binaural neurons in the time pathway presumably have a characteristic delay, although they also respond to time disparities that are removed from the characteristic delays by n periods of the neuron's best or stimulus frequency. However, at the final stage of time coding the space-specific neurons respond exclusively to the interaural time differences equivalent to their characteristic delays.

Indirect evidence supports the hypothesis that the nucleus laminaris contains a map of phase equivalents of characteristic delays. In the central nucleus of the inferior colliculus, one of the projection areas of the nucleus laminaris, the phase equivalents of characteristic delays are also mapped. Phase-sensitive neurons of the central nucleus are arranged such that a columnar array of them across isofrequency laminae represents a single characteristic delay. This column of neurons appears to project onto a space-specific neuron in the external nucleus of the inferior colliculus; the projection pattern confers upon a space-specific neuron its broad frequency tuning and ability to signal the characteristic delay unambiguously. The connectivity also explains how a nontonotopic

map of auditory space is derived from tonotopically organized lower-order nuclei. Reunion of the time and intensity pathways in the inferior colliculus gives rise to the selectivity of space-specific neurons for a particular combination of the binaural cues, which corresponds to a location in auditory space. Space-specific neurons form a two-dimensional map of auditory space in the external nucleus.

Few attempts to carry out a systematic study of stimulus processing throughout the auditory system have been successful. The belief that one must start from the periphery and go "upstream," characterizing the transfer function of each relay station, is one reason for this lack of success. The nonlinear nature of neural processing, combined with code transformation, seldom permits a logical prediction of the transfer function of a higher-order station from that of a lower-order station. Furthermore, higher-order stations may be progressively more specialized for processing biologically significant or natural stimuli. Therefore, the use of natural stimuli might enable one to penetrate farther upstream than one can with artificial stimuli such as tones. In vertebrates, the work on electric fish is the only example in which the upstream approach has led to a reasonable explanation of the relevant behavior in terms of the roles played by different levels of neural organization. Knowledge of natural stimuli and their detection by the fish is indispensable for the success of the approach (Heiligenberg and Bastian, 1984).

Is a "top-down" or "downstream" approach—that is, going from higher- to lower-order neurons—possible? A higher-order neuron's selectivity for a complex stimulus is usually difficult to explain in terms of the response properties of lower-order neurons (Marr, 1982). Nevertheless, the stimulus selectivity of a complex neuron is largely shaped by its afferents, and it should, therefore, be possible to trace the components and causes of the selectivity to lower-order neurons in the afferent pathways. Another common objection to the use of higher-order neurons as a starting point for systematic analysis is the belief that complex neurons are isolated oddities. However, in many well-documented cases, such as specialized areas in the auditory cortex of the mustached bat *Pteronotus parnellii* (Suga, this volume), the torus semicircularis of the electric fish (Heiligenberg and Rose, 1985), the inferotemporal cortex in the macaque's visual system (Gross, 1973; Perrett et al., 1982), and the space-mapped region of the owl's inferior colliculus (IC) (Knudsen and Konishi, 1978a,b), neurons requiring complex stimuli are the rule rather than the exception. The use of natural signals may facilitate the discovery of complex neurons. Therefore, "biologically relevant" stimuli are desirable for both the up- and downstream approaches.

Only behavioral studies can show what stimulus is significant to the animal. The behavioral relevance of a stimulus is important not only for the design of experiments but also for the interpretation of physiological and anatomical observations. The work reviewed in this chapter presents an example of integrating behavior, physiology, and anatomy into a unified research strategy. The outcome of this approach enables us to provide a reasonable explanation for the owl's ability to use binaural cues in sound localization.

THE BEHAVIORAL CHARACTERIZATION OF AUDITORY SPACE

The choice of animals is especially important for behavioral analysis. Animals for which sound signals are important tend to show natural responses that can be exploited for psychoacoustical tests. The barn owl (*Tyto alba*, hereafter referred to as the owl) is such an animal. The owl is particularly suitable for the study of sound localization because of its exquisite ability to track sound. The owl aligns its head to the source of sound in a stereotyped manner (Knudsen and Konishi, 1979; Knudsen et al., 1979). The accuracy of head orientation relative to the target serves as a good measure of localization acuity. Sound delivered through earphones also elicits the head-turning response, allowing the analysis of localization as a function of dichotic stimulus variables. These studies show that the owl uses interaural time differences (ITDs) for localization in the horizontal plane or azimuth and interaural intensity differences (IIDs) in the vertical plane or elevation (Moiseff and Konishi, 1981, and unpublished observations). Therefore, the owl's two-dimensional auditory space is defined by a matrix of the two binaural cues.

Space-Specific Neurons

Free-field studies with a movable sound source revealed that neurons in the owl's MLD [nucleus mesencephalicus lateralis, pars dorsalis; homologous to the IC (Knudsen, 1983)] respond only to sound emanating from a particular direction. These neurons, termed space-specific neurons, are arranged in an orderly topographic sequence, forming a map of auditory space in the external nucleus of the inferior colliculus (ICX) (Knudsen and Konishi, 1978a,b). Experiments with earphones show that each space-specific neuron is selective for a particular combination of time and intensity disparities. These neurons are also exclusively binaural; they cannot be driven by monaural stimuli. Another attribute that distinguishes them from neurons in the central nucleus of the inferior colliculus (ICC) is broad-frequency tuning. Many space-specific neurons respond to frequencies between 3 and 9 kHz.

The relationships between a neuron's dichotic stimulus requirements and its receptive field were established by a combination of free-field and dichotic methods of stimulation. While recording from a single space-specific neuron, the neuron's spatial receptive field was determined with a free-field stimulus. Earphones were then inserted into the external auditory canal to determine the neuron's tuning to time and intensity disparities (Moiseff and Konishi, 1981). Measurements of time disparities generated by free-field stimuli using microphones placed near the eardrums showed that the azimuthal center of a receptive field corresponds to the sound incidence angle that creates the optimal time disparity for the neuron. Partial occlusion of one ear, which alters intensity disparity, causes a shift mainly in the vertical coordinate of a receptive field (Knudsen and Konishi, 1980). These observations suggest that the tuning of a space-specific neuron to a particular combination of time and intensity disparities determines the azimuthal and elevational coordinates of its receptive field, respectively (Figure 1).

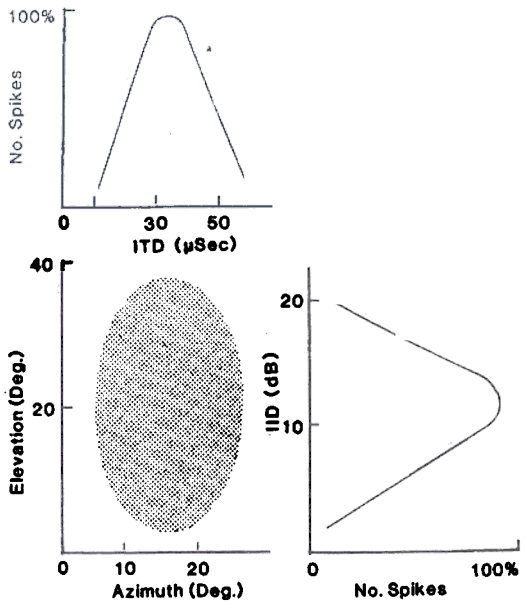

Figure 1. *Binaural cues for receptive fields.* A space-specific neuron requires binaural stimuli containing a particular combination of ITDs and IIDs. This diagram is a scale model of a neuron's receptive field (*shaded area*) and its ITD and IID tuning curves.

SEPARATE PATHWAYS FOR TIME AND INTENSITY

The space-specific neuron's selectivity for binaural disparities can be traced back to lower-order nuclei. A complete survey of brain-stem binaural nuclei showed that they can be divided into two groups, one with neurons sensitive to time disparity and the other with neurons sensitive to intensity disparity (Moiseff and Konishi, 1983). Each group forms an anatomically distinct pathway that starts from one of the cochlear nuclei, the nucleus magnocellularis (NM) for the time pathway and the nucleus angularis (NA) for the intensity pathway (Figure 2) (Moiseff and Konishi, 1983; Takahashi and Konishi, 1988a,b).

Recent studies show that an immunohistochemical reaction can distinguish the time pathway from the intensity pathway (Carr et al., 1985). Antibodies against vitamin D-dependent calcium binding protein (CaBP) bind more heavily and uniformly to neurons in the eighth nerve, NM, and NL than to neurons in the NA. Also, CaBP-labeled axon terminals allow the lemniscal and midbrain projection areas of the NL to be distinguished from those of the NA.

Time and intensity cues are processed independently in the two parallel pathways (Takahashi et al., 1984). This conclusion derives from an experiment that analyzed the effects of partial inactivation of one cochlear nucleus (CN) on the time and intensity selectivity of space-specific neurons. Injection of a local anesthetic, lidocaine, into the NA causes a reversible shift and broadening of a space-specific neuron's selectivity for intensity disparity without affecting its

selectivity for time disparity (Figure 3). The converse occurs when the NM is partially inactivated, that is, selectivity for time is affected and selectivity for intensity is unaffected (Figure 4).

Functional Segregation in the Cochlear Nucleus

In parallel with the different effects of inactivating the CN, distinct physiological and anatomical differences separate the two nuclei. Neurons in the NM tend to fire at a particular phase angle of a tonal signal. This phenomenon is known as "phase locking." Although a neuron cannot follow a high-frequency signal cycle by cycle, when it does fire, it fires most often at a particular phase angle. The high-frequency limit of phase locking in the CN is about 3–4 kHz in laboratory mammals (Lavine, 1971; Rose et al., 1974). In the owl's NM phase locking can occur at frequencies as high as 8–9 kHz (Sullivan and Konishi, 1984). Neurons

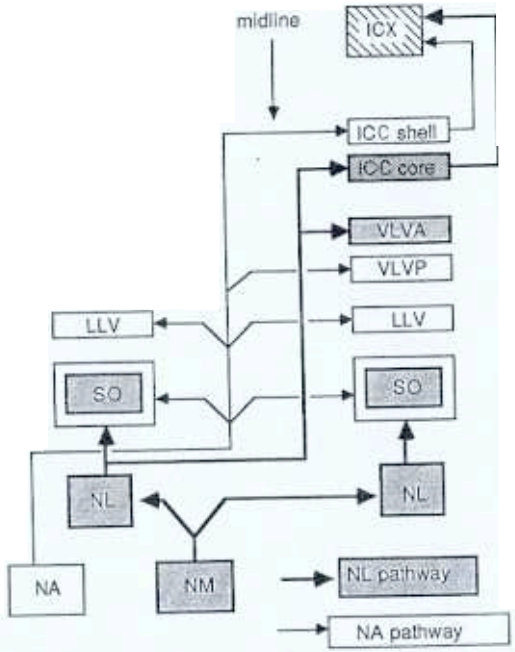

Figure 2. *Projections of the cochlear nuclei (NM and NA) and NL of the barn owl.* NM, the neurons of which encode the phase angles of the spectral components of sounds arriving in the ipsilateral ear, projects solely and bilaterally to NL. Thus NM and NL are, respectively, the first and second stations of the time pathway. NM and the higher-order nuclei innervated by NL are enclosed in *shaded boxes*. NA, the neurons of which encode the intensity of sounds arriving in the ipsilateral ear, projects directly to higher auditory centers such as the lateral lemniscal nuclear complex and inferior colliculus. Its projections are enclosed in *unshaded boxes*. The superior olive (SO) is innervated by both NA and NL. The external nucleus of the inferior colliculus (ICX, *crosshatched box*) is innervated by neither NA nor NL. The *downward-pointing arrow* at the *top* indicates the position of the midline.

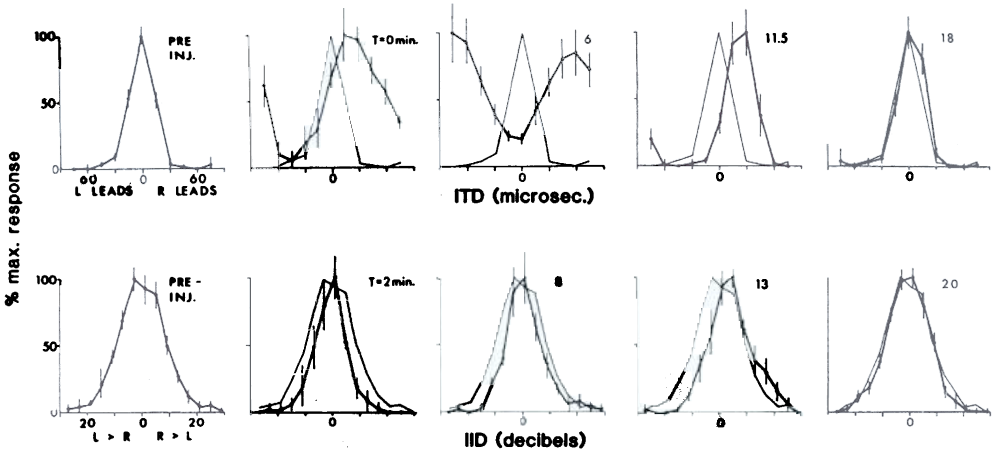

Figure 3. *Injection of lidocaine, a local anesthetic, into the NM alters a space-specific neuron's selectivity for ITDs but not its selectivity for IIDs.* Before lidocaine injection (Pre-inj.), the cell is selective for noise stimuli of equal intensities presented simultaneously to the ears (IID = 0 dB; ITD = 0 μsec). Upon injection (T = 0 min), the cell becomes responsive to the previously ineffective ITD values (T = 0 min to T = 6 min), then recovers over the next 12 min (T = 6 min to T = 18 min). Its selectivity for IID remains unchanged throughout. The graph of the neuron's response to ITD and IID obtained prior to lidocaine injection is superimposed on each of the other graphs for easy comparisons in this figure and Figure 4. Neuronal responses are expressed as normalized discharge rate.

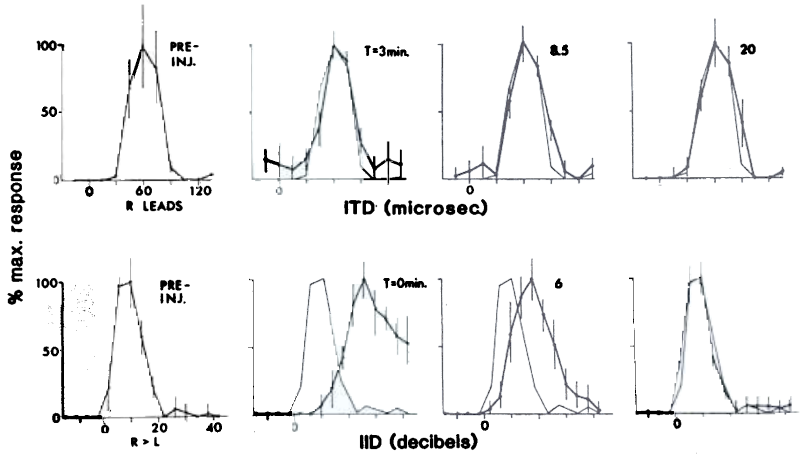

Figure 4. *Injection of lidocaine into the NA alters a space-specific neuron's selectivity for IID, but not its selectivity for ITD.* Prior to lidocaine injection, the neuron responds best when the noise stimulus in the right ear leads by 60 μsec and is 12 dB louder. Upon injection, the neuron becomes less selective and responds best when the noise stimulus in the right ear is 22 dB louder. It regains its sharp selectivity to the original IID in the ensuing 15 min. Meanwhile, the neuron's selectivity for ITD is unchanged.

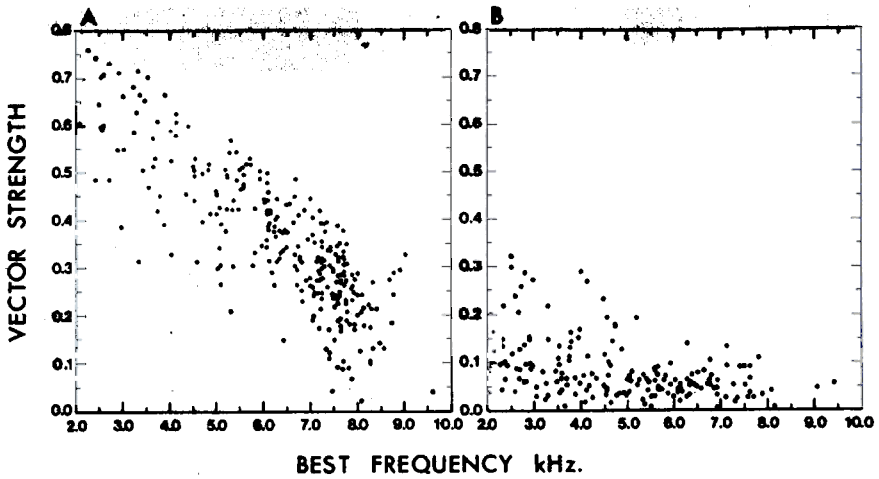

Figure 5. *Differences in phase locking between the cochlear nuclei.* The degree of phase locking, vector strength calculated according to the method of Goldberg and Brown (1969), is plotted as a function of BF for 296 NM neurons (*A*) and 179 NA neurons (*B*). The vector strength is measured for a given neuron at its BF and 20 dB above threshold. A value of one indicates perfect phase locking, while zero indicates random discharge with reference to stimulus phase. The vector strengths of NM neurons are greater than those of NA neurons for frequencies up to about 9 kHz. The vector strengths of NA neurons are usually less than 0.1, and these values can be explained by random spike distributions rather than by low levels of phase locking.

in the NA fail to phase-lock or do so poorly, even at low frequencies (Figure 5) but are more sensitive to variation in stimulus intensity than are NM neurons. These observations provide support for the hypothesis that the NM is specialized to process phase information, whereas the NA is specialized for intensity processing.

Two conspicuous anatomical differences appear to be correlated with some of the physiological differences. Each primary auditory fiber divides into two collaterals, one terminating as large calycine endings on the somata of the NM and the other in synaptic boutons in the NA (Figure 6). NM neurons (especially those sensitive to high frequencies) have very few dendrites, whereas NA neurons are stellate. These differences in pre- and postsynaptic morphology should produce very different response properties (Molnar and Pfeiffer, 1968).

The morphological and physiological differences seen in the owl's CN are similar to the distinction between bushy cells of the anteroventral cochlear nucleus (AVCN) and stellate cells of the posteroventral cochlear nucleus (PVCN) of mammals. The intracellular staining of physiologically identified cells in the cat CN shows that neurons having a primarylike discharge pattern most often correspond to bushy cells with calycine terminals, whereas neurons having a chopper discharge pattern correspond to multipolar or stellate cells with boutonal endings along their dendrites (Rhode et al., 1983; Oertel et al., this volume).

We believe that NM neurons are similar to the bushy cells, for both types of neurons show phase locking, have primarylike discharge patterns (Sullivan,

1985), receive calycine terminals from VIIIth nerve fibers (Carr et al., 1985; Takahashi and Konishi, 1988a) and have large somata with limited dendritic arbors. NA neurons are similar to the stellate cells of the mammalian ventral cochlear nucleus (VCN). Both types show little or no phase locking, have chopper response patterns indicating a very regular pattern of discharge, and have similar morphological characteristics at both the presynaptic and postsynaptic levels (Sullivan, 1985). The similarities between neurons in the barn owl's CN and identified cell types in the mammalian VCN lead us to suspect that the functional segregation with respect to time and intensity processing seen in the barn owl may be a general property of the CN in birds and mammals.

The pathway separation above the owl's CN may also have a counterpart in mammalian systems: Each cell type in the VCN has a unique pattern of projections (Warr, 1982; Young et al., this volume). The major difference between mammals and owls is that in mammals, the segregation of time and intensity pathways appears to be by frequency, namely low-frequency channels for time and high-frequency ones for intensity.

FURTHER STAGES OF TIME CODING

We devote the rest of this chapter mainly to the discussion of the neuronal processes underlying the measurement and encoding of time disparities, because

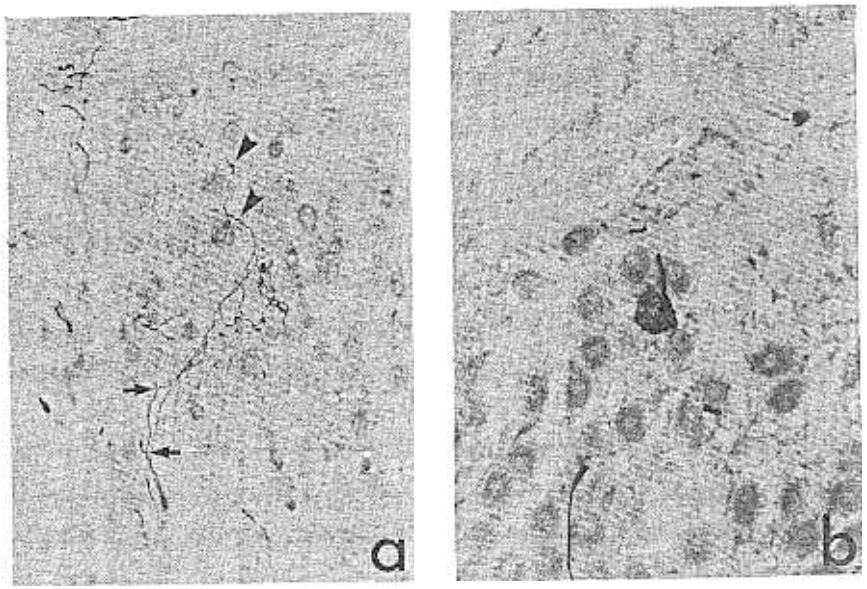

Figure 6. *Differences in synaptic terminal in the CN.* VIIIth nerve terminals typical of the NA (*a*) and NM (*b*). In the NA, VIIIth nerve collaterals branch repeatedly and form boutonal synapses on and in the vicinity of somata and dendrites. In the NM, VIIIth nerve collaterals terminate as large calycine endings which appear to grasp the postsynaptic neuron.

we know more about the successive stages of time coding than about those of intensity coding. Before proceeding, it is useful to explain the concepts and terms concerning the encoding of time. A dichotically presented tone burst contains two kinds of cues for the measurement of ITDs and transient time and phase disparities. Transient time disparity refers to a difference in the arrival of the first wave of the signal between the ears. Phase disparity refers to a difference in the arrival of a given phase angle between the ears. A dichotic noise burst also provides transient time cues. However, an interaural phase difference (IPD) cannot be assigned to a noise waveform, because different spectral components of the noise have different period lengths. For this reason, the term ongoing time difference, as contrasted to transient time difference, has been used to describe the disparities in the internal timing of a noise waveform (Moiseff and Konishi, 1981).

All binaural neurons in the time pathway are sensitive to variation in IPD. However, they are tuned not to phase disparity but to time disparity. Phase ($\Delta\phi$) and time (Δt) disparities have the relationship $\Delta\phi = 2\pi\Delta tF$, where F is frequency. Therefore, if a neuron is selective for an IPD as such, it should prefer the same phase difference regardless of frequency. On the other hand, if a neuron is selective for ITDs, it should prefer the same time disparity independent of frequency. This time disparity is the neuron's characteristic delay (CD) (Rose et al., 1966; Goldberg and Brown, 1969). Evidence suggests that all binaural neurons in the time pathway have CDs. However, they also signal time disparities that are removed from their characteristic delays by n periods of their best frequencies (BFs) (phase equivalents of their CDs). These time disparities will be referred to as virtual time disparities. This phenomenon, a consequence of using phase to measure time, occurs whether the stimulus is a tone or a noise, because the neurons are tuned to a narrow band of frequencies. The neurons cannot distinguish the particular dichotic pair of cycles containing the phase equivalent of their preferred time disparity from other pairs containing the recurrent values of the phase difference.

The further stages of time coding include the measurement and encoding of time disparities in the NL—the first site of binaural convergence—the transfer of time disparity codes to higher-order stations, the enhancement of neuronal selectivity for time disparities, and the elimination of responses to virtual time disparities by the convergence of different frequency channels onto space-specific neurons.

Measurement and Encoding of Interaural Time Difference: A Model

Phase-locked spikes encode the timing of the stimulus. The owl's auditory system uses this code for the measurement of time disparity. Jeffress (1948) put forth an ingenious model to explain the measurement as well as the encoding of time disparities by neuronal circuits. We first discuss the essence of his theory and then present anatomical and physiological evidence which suggests that the NL uses neuronal circuits similar to the Jeffress model for the measurement and encoding of time disparities. Although Jeffress' model differs from that shown in Figure 7, the principles involved are the same; that is, both models consist of delay lines and coincidence detectors. In Figure 7, neurons A, B, C, D, and

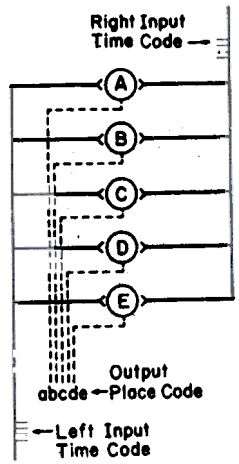

Figure 7. *Model of neural circuits for measuring and encoding ITDs.* The principles used are delay lines and coincidence detection. The binaural neurons A, B, C, and so on fire maximally when signals from the two sources arrive simultaneously, thus serving as coincidence detectors. Temporal information such as phase is encoded in the timing of spikes. The model uses different axon lengths to vary delays in signal transmission. The axonal path to the neurons (*thick lines*) increases systematically along the array but in the opposite directions for the two input channels. This pattern of innervation creates left–right asymmetries in transmission delays. When binaural disparities in acoustic signals exactly compensate for these asymmetries, the neurons fire maximally. The outputs of the neurons, as indicated by *dotted lines*, do not use the timing of spikes for encoding time. Only the place of a neuron in the array can signal the ITD to which the neuron responds maximally.

E, which are arranged in a columnar array, fire maximally when neural signals from the left and right input channels arrive simultaneously. The axons from the left and right sources innervate the neurons sequentially from the opposite ends of the array. Thus the length of the axonal path to the neurons increases systematically from top to bottom for the right channel and from bottom to top for the left channel. This pattern of innervation gives rise to unequal axonal paths from the two sources for most of the neurons in the array. Being coincidence detectors, the neurons with unequal left and right paths respond maximally only when the timing of the stimulus is adjusted for the simultaneous arrival of the spikes coding for the stimulus timing. Such an adjustment requires the selection of a particular time disparity. In other words, each neuron is tuned to a single time disparity, and different neurons are selective for different disparities.

The input signals to the coincidence detectors in our model are encoded in the timing of spikes, but their outputs use neither spike time nor rate for encoding time disparities. In this case, the only code that can represent a time disparity is the place of a neuron in the array. In Figure 7, the outputs of the coincidence detectors A, B, C, . . . are labeled by a, b, c, . . ., respectively. The array conveys the pattern of discharge among different labeled lines to the next array.

The Anatomic Characteristics of the Nucleus Laminaris

The NL, which is similar to the medial superior olive (MSO) of mammals, receives bilateral inputs exclusively from the NM. The tonotopic organization of the NM projects topographically onto the NL (Parks and Rubel, 1975; Takahashi and Konishi, 1988a). This nucleus in the owl is vastly expanded from the monolayer structure typical of other birds such as pigeons and chickens (Figure 8) (Parks and Rubel, 1975; Boord, 1978). It contains five times more neurons than the NL of other birds of similar size (barn owl, 10,020 vs. crow, 2540; Winter and Schwartzkopff, 1961). The owl's NL neurons have large cell bodies (30–40 μm)

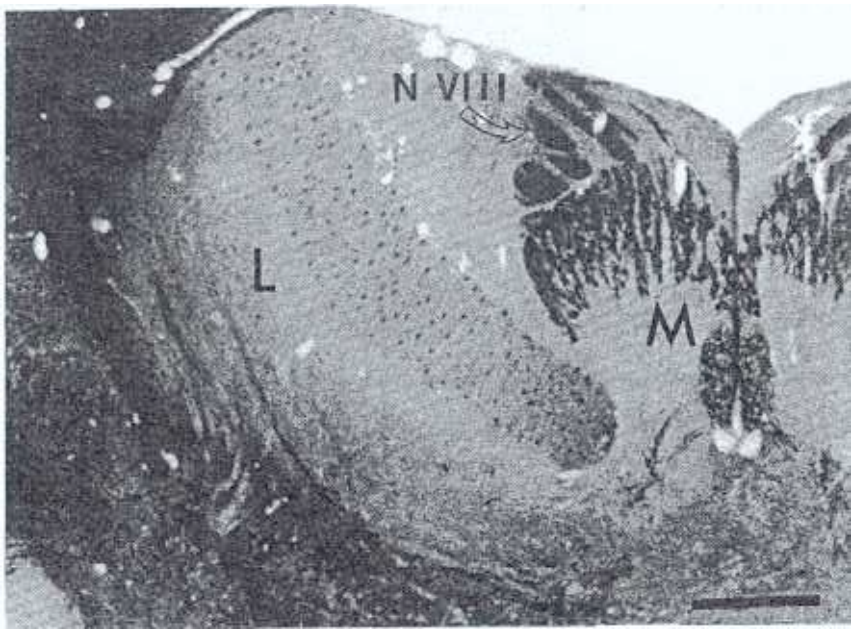

Figure 8. *Distribution of cell bodies in the NL.* A coronal section stained with antibodies against vitamin D-dependent calcium binding protein (CaBP). The heavily stained VIIIth nerve is marked with an *arrow* where it descends into the NM (M). The NL contains approximately 10,000 large (30–40 μm) neurons, which are sparsely but evenly distributed in a central neuropil area. These cells have many short, stubby dendrites and/or somatic spines which range from 10 to 50 μm in length. The dendrites of these neurons do not extend farther than a cell diameter from the soma. *Calibration bar* = 500 μm.

and conspicuous somatic spines and/or stubby dendrites. These neurons are sparsely but regularly distributed in a plexus of myelinated fibers. Incoming axons from the ipsilateral NM travel along the dorsal border of the nucleus, while axons from the contralateral NM travel on the ventral border until they reach their specific isofrequency lamina; there each axon divides into thinner collaterals which enter the NL. Once inside the NL each collateral immediately divides into 2–4 branches of similar thickness that travel through the neuropil along a course almost perpendicular to the dorsal and ventral surfaces (Figure 9). Some branches course through the NL and terminate on the neurons close to the opposite surface. The fibers have many prominent nodes; some nodes are the origin of short, thin collaterals that terminate as blunt, club-shaped endings closely apposed to the neurons (Carr et al., 1985).

The Response Characteristics of Single Nucleus Laminaris Neurons

Although recording from single NL somata is difficult, their axons in the output tract can be isolated for recording. Spikes in these axons are phase-locked to monaural stimuli. The phase of a tonal stimulus or of a noise spectral component

at which an NL neuron shows a maximal firing probability can be different depending on which ear is stimulated (Figure 10A). This phenomenon suggests that phase-locked discharge of an NL neuron takes a longer time to elicit from one side than from the other side. This asymmetry in the timing of the phase-locked discharge will be termed binaural delay disparity (BDD). An NL neuron's selectivity for time disparity appears to be causally related to its binaural delay disparity, for it fires maximally when an asymmetry in acoustic transmission time nullifies its BDD (Figure 10B). In other words, an NL neuron has a CD that is of the same magnitude as its BDD but opposite in sign. For example, the neuron in Figure 10A and B showed a constant BDD of approximately 40 μsec (left leading right) for all three frequencies tested, and the neuron fired maximally when the right side led the left side by 40 μsec. This finding suggests that, like MSO neurons, NL neurons act as coincidence detectors (Goldberg and Brown, 1969; Sullivan and Konishi, 1984). However, it should be noted that coincidence detection is not all or nothing but graded. A neuron's most preferred time disparity elicits a maximal response, and suboptimal time disparities elicit reduced responses. Also, NL neurons respond maximally to virtual time disparities as well. Thus these neurons signal the phase equivalents of their CDs.

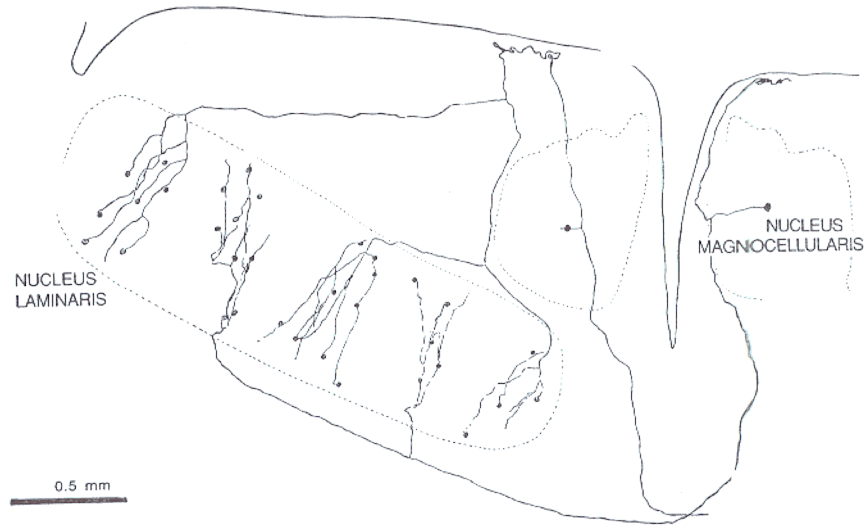

Figure 9. *Innervation of the NL.* This figure shows a reconstruction of afferents labeled after an HRP injection in the NM. Each NM axon bifurcates to innervate the NL bilaterally. The zone of innervation represents the same frequency in the two NL nuclei. The axon travels along the surface of the NL and gives off branches that penetrate the target zone. Collaterals from the ipsilateral NM enter the dorsal surface. They interdigitate with collaterals from the contralateral NM, which enter ventrally. The collaterals are thinner than the main axon trunk and have simple branching patterns and many nodes. Each NM neuron may contact 10–20 NL neurons on each side. The NM axon terminals, which are large and club shaped, end closely apposed to the NL neurons. Many collaterals also appear to contact the NL somata by short branchlets. *Calibration bar* = 1 mm.

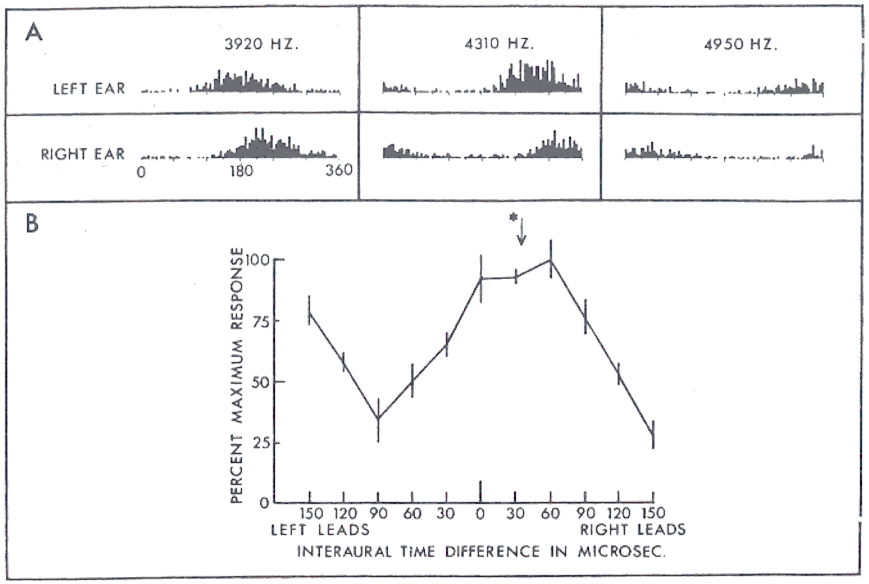

Figure 10. *Binaural delay disparity and coincidence detection.* The NL is the first site of binaural convergence in the time pathway. An NL neuron phase-locks to tonal stimuli presented to either ear. *A*: A neuron's period histograms obtained for three different frequencies. The number of spikes (*ordinate*) is plotted against phase angles (*abscissa*). Note that, for all frequencies, the peak in the right ear histogram is displaced (by about 40 μsec) from that in the left ear histogram. This asymmetry indicates that phase-locked spikes take a longer time to be elicited from the right ear than from the left ear. *B*: Laminar neurons also fire maximally in response to a particular ITD and its phase equivalents. In the example above, maximal discharge occurred when the right ear stimulus led the left one by 40 μsec (*arrow*), which offsets the asymmetry. Hence, NL neurons appear to work as coincidence detectors.

A Frequency and Time Map of Evoked Potentials in the Nucleus Laminaris

The difficulty of isolating NL somata for recording makes it impossible to determine whether or not neurons having different BDDs are systematically distributed. However, we could obtain indirect evidence for a map of delays by using an evoked potential known as a "neurophonic." A tonal stimulus evokes a nearly sinusoidal neurophonic with a frequency identical to that of the stimulus (Weinberger et al., 1970; Snyder and Schreiner, 1984).

The frequency selectivity of the neurophonic changes little during a penetration along the dorsoventral axis of the nucleus. By contrast, the phase of a monaurally evoked sinusoidal neurophonic shifts as a function of recording site within each isofrequency lamina (Figure 11). Furthermore, ipsi- and contralateral ear stimulation results in opposite phase shifts along the dorsoventral axis; for ipsilateral stimulation the phase delay increases with depth, and for contralateral stimulation it decreases. These opposite shifts give rise to a different left and right phase disparity for each recording site. The time equivalents of these disparities range from 0 to about 180 μsec, corresponding to the range of time disparities experienced by

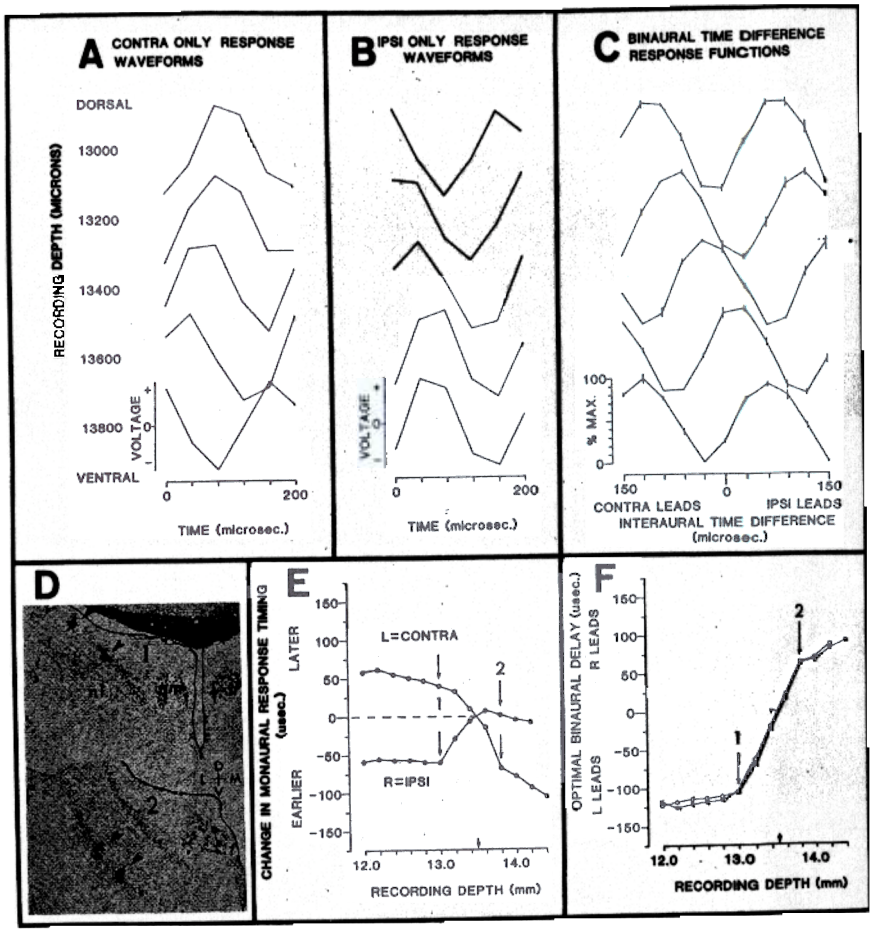

Figure 11. *Map of transmission delays in the NL.* The NL generates a large evoked potential with waveform and frequency similar to the tonal stimulus used. This signal is termed a neurophonic, or frequency-following, potential. *A*: Neurophonic evoked by the stimulation of the contralateral ear shows a gradual decrease in phase delay with the depth of the recording site, as shown with one cycle of 5-kHz waveform. *B*: Direction of the site-dependent phase shifts is reversed for ipsilateral ear stimulation. Binaurally evoked neurophonics vary as a function of ITD. At each recording depth, an ITD and its phase equivalent elicit a maximal amplitude in neurophonics, and the optimal binaural delay varies systematically, as shown in *C*. *D*: Coronal sections of the NL. Lesions in *1*, as denoted by *arrows*, indicate the dorsal surface, where a linear change in the optimal binaural delay begins. Lesions similarly denoted in *2* indicate the ventral surface where the linear change ends. *E*: Change in the timing of monaurally evoked neurophonics with depth. At each depth, the monaural waveform was cross-correlated with the first monaural waveform recorded in the penetration. Time zero is arbitrarily set to the depth at which the two waveforms are in phase. *F*: Change in the optimal binaural delay as a function of depth. *Arrows 1* and *2* mark the depths at which the lesions were placed in *1* and *2* in *D*, respectively. Note that the plot of time differences between left and right monaural waveforms against depth (*circles*) closely matches the plot of optimal binaural delays (*squares*).

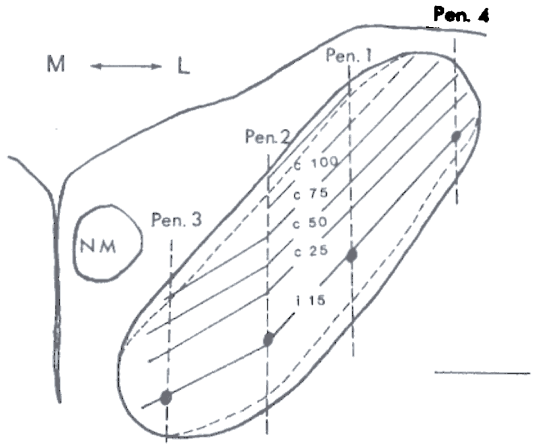

Figure 12. *Contour map of neurophonic delays in the NL.* The phase of a sinusoidal neurophonic changes systematically with the recording depth; it advances for contralateral ear stimulation and lags for ipsilateral ear stimulation. Left and right neurophonics show a phase difference at each recording depth. When this phase difference is offset by an appropriate shift in stimulus timing, the neurophonic attains a maximal amplitude. This time shift varies systematically along the dorsoventral axis of the nucleus. The contour lines connect the loci where the same time shifts were required in four different penetrations (Pen. 1, 2, etc.). c 100, c 20, and so on denote the tone to the contralateral ear leading the tone to the other ear by 100 and 20 μsec, respectively. Abbreviations: i, ipsilateral ear leads; M, medial; L, lateral; NM, nucleus magnocellularis. *Calibration bar* = 500 μm.

the owl (Figure 12). The neurophonic phase disparity varies systematically along the dorsoventral axis of the nucleus. Furthermore, binaural neurophonic potentials attain a maximal amplitude in response to a particular time disparity. The time difference computed by cross-correlation of the left and right neurophonic potentials for each recording site equals the time disparity optimal for that location. The optimal binaural delay, which varies with recording depth, is such as to equalize ipsi- and contralateral phase delays for any given site, causing the two monaural waveforms to be in synchrony with each other.

NL neurons receive inputs from the NM which are sharply frequency-tuned, and thus a time disparity in a noise signal must be derived from phase disparities in separate spectral components of the noise. The derivation of an ITD from binaural phase comparison requires the matching of ipsi- and contralateral input frequencies, because a given binaural phase difference corresponds to different time disparities for different frequencies. NL neurons satisfy the above condition, because their ipsi- and contralateral inputs are tuned to the same narrow frequency range. The division of the NL into separate frequency channels also requires a complete library of BDDs in each frequency channel. Neurophonics show that a complete range of delays is present in many isofrequency bands.

A Delay-Line Model of the Nucleus Laminaris

We propose a model of the NL that can account for all the anatomical, single neuron, and neurophonic observations mentioned above. We use direct and

indirect lines of evidence to argue that the NL uses the principles of delay line and coincidence detection for the measurement of time disparities, that the place of an NL neuron codes for the phase equivalent of a time disparity, and that the NL contains a map of phase equivalents of time disparities. The response of NL axons provides evidence for coincidence detection and the presence of asymmetrical transmission delays (BDDs). We assume that the neurophonic data show a systematic distribution (map) of transmission delays. This assumption holds whether the neurophonic originates from NL somata or in the incoming NM axons; the observed shifts of neurophonic phase suggest that the arrival of phase-locked spikes is systematically delayed as a function of distance from either surface of the nucleus. The innervation pattern of the NL provides indirect evidence for the assumption that the systematic variation in transmission delays is due to the systematic changes in the axonal paths to NL somata. If this assumption is correct, it follows that NL neurons are systematically arranged (mapped) according to their CDs.

Our model of the NL resembles the one in Figure 7. Asymmetric neural delays caused by opposing delay lines and coincidence detection underlie an NL neuron's selectivity for a specific time disparity. The ipsi- and contralateral NM fibers innervate sequential arrays of neurons serving as coincidence detectors. The length of the ipsilateral path to a neuron increases in the dorsoventral direction, whereas the contralateral path increases in the opposite direction. If one were to record from the array neurons, one would expect that movement in a ventral direction should result in a longer delay from the ipsilateral side and a shorter delay from the contralateral side. Neurons in more ventral locations should thus be tuned to time disparities in which the ipsilateral ear is stimulated slightly earlier to compensate for the extra neural delay from the ipsilateral side.

The idea of place coding by NL neurons needs to be clarified, because their phase-locked discharge might provide a code for time disparity. Neither the timing nor the rate of discharge of an NL neuron can encode time disparity uniquely, because a given time disparity may elicit the same rate and timing pattern of discharge in neurons tuned to different time disparities. Similarly, the maximal discharge rate cannot uniquely encode the optimal time disparity, because neurons selective for different disparity values may have the same maximal rate. Therefore, NL neurons must use means other than the rate or timing of spikes for encoding time disparities. The only remaining means is "place."

Projection of the Place Code

The NL projects to a restricted zone in the contralateral ICC. In this nucleus, single unit mapping of neuronal properties revealed an orderly distribution of neurons according to their selectivity for frequency and time disparity. Neurons in the ICC also signal the phase equivalents of their CDs. As in the NL, the response of a neuron in the ICC varies as a function of time disparity. This function is a cyclic curve with multiple response maxima that are separated by a period equal to that of the stimulus tone. Systematic sampling of neurons within an isofrequency lamina shows that the neurons occur in an orderly sequence according to their preferred phase disparities (Figure 13). Neurons recorded during one penetration across isofrequency laminae yield curves with periods

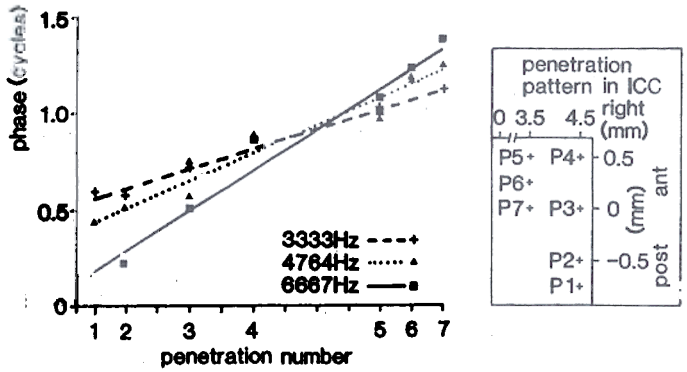

Figure 13. *Map of mean interaural phase in each isofrequency lamina of the ICC.* A series of penetrations covering the entire time-sensitive area of the ICC reveals a gradual change of mean interaural phase with the position of the penetration. As is indicated in the panel on the *right*, penetrations P1 to P7 were made along a hooklike contour: P1 to P4 along the lateral margin of the nucleus and P5 to P7 along the medial margin. The origin of the coordinate system refers to the intersection of the interaural axis with the midline of the skull. The mean interaural phase ($\bar{\phi}$) was calculated from response curves similar to those of Figure 14 and denotes the phase value (in fraction of the period of the stimulus) around which the response is centered. The graph to the *left* shows systematic changes in mean interaural phase as a function of the recording site for three isofrequency laminae.

corresponding to their BFs. All of the curves reach a maximum at only one particular time disparity, the positions of other maxima varying with frequency (Figure 14) (Wagner et al., 1987). This neuronal array possesses attributes associated with the CD, such as the linear relationship between mean interaural phase and frequency (Yin and Kuwada, 1983). Thus a vertical array of neurons in the ICC behaves as if it had a single CD. Hence, the direction in which time disparity tuning changes in the ICC appears to be perpendicular to that of frequency.

Each NL neuron or locus is tuned to both frequency and time disparity. In the ICC, the best frequency increases monotonically from dorsal to ventral (Knudsen and Konishi, 1978a). This tonotopic sequence is consistent with the pattern of neuronal projection from the NL to the ICC (Takahashi and Konishi, 1988a). Moreover, in both nuclei, the direction of change in time disparity tuning is also approximately perpendicular to that of frequency. All of the observations mentioned in this section, taken together, suggest that the NL map of phase equivalents of CDs projects topographically onto the ICC.

The study of connections between the ICC and ICX shows that a single locus in the ICX receives inputs from neurons distributed over different isofrequency laminae (Knudsen, 1984a). These neurons are now known to form a columnar array representing a single CD. An injection of horseradish peroxidase (HRP) into a restricted area of the ICX having a known CD labels a vertical column of neurons in the ICC representing the same CD. Thus the vertical arrays in the ICC representing a CD in many narrowly frequency-tuned neurons appear to constitute the input stage to one broadly frequency-tuned neuron in the ICX representing the same CD (Wagner et al., 1987).

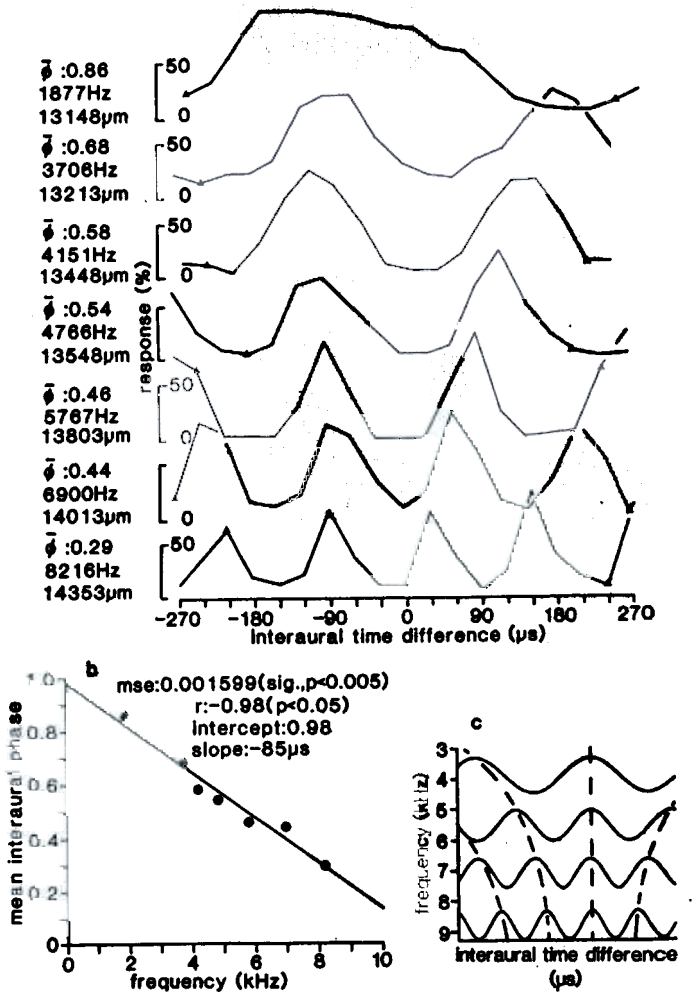

Figure 14. *Coding of an ITD by an array of neurons in the ICC. a*: Array of seven recording sites obtained in one dorsoventral penetration. Recording depth, BF, and mean interaural phase at each site are indicated on the *left*. The panel shows the normalized response curves to stimulation with interaural differences (five repetitions/stimulus) delivered at each unit's BF. $\bar{\phi}$ denotes the mean interaural phase measured from the response curves between the points spanned by the *triangles* and was calculated as mentioned in Figure 13. *b*: Dependence of mean interaural phase on stimulus frequency at different recording sites. There is a statistically significant linear relation between these variables, as indicated by both the correlation coefficient *r* and the mean square error. The *slope* of the regression line has the unit of time. Its value gives the CD or ITD by the vertical array of neurons in this penetration. *c*: A schematic version of *a*.

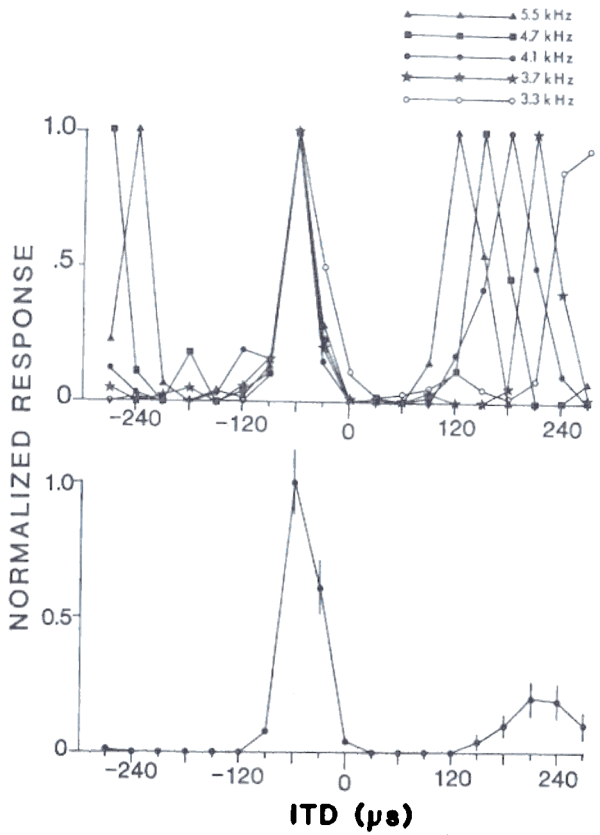

Figure 15. *Neuronal selectivity for CD.* Response curves from a space-specific neuron obtained by stimulation with tones (*top*) and noise (*bottom*). The response of a space-specific neuron to tonal stimuli is a cyclic function of ITD. The period of each response curve is that of the stimulus tone (*top*). One ITD, −60 μsec for the neuron depicted above, elicits a maximum discharge regardless of the frequency of the stimulus tone (*top*). This ITD is the unit's CD. When the stimulus is noise, there is a maximal response only at the CD (*bottom*).

Neuronal Selectivity for Characteristic Delay

The pattern of projection from the ICC to the ICX underlies the space-specific neuron's ability to signal a single time disparity (Figure 15). Unlike neurons in the NL, the anterior portion of the nucleus ventralis lemnisci lateralis (VLVA), and the ICC, space-specific neurons show no cyclical responses to noise, their responses to virtual time disparities being completely or largely suppressed. The use of a sound composed of two discrete frequencies enabled us to demonstrate that the effects of noise can be explained by nonlinear interactions between different frequency channels converging on a space-specific neuron (Takahashi and Konishi, 1986). The response to the CD is facilitated beyond levels obtained by stimulation with either of the two frequencies alone, and the response to the virtual time disparities is inhibited.

The sharpened selectivity for time disparity is another attribute that distinguishes space-specific neurons from lower-order neurons. However, unlike the solution of phase ambiguity, the enhancement does not seem to require more than one frequency channel, for the tuning of space-specific neurons to time disparity is as sharp with a tone as with a broadband noise.

A TWO-DIMENSIONAL MAP OF AUDITORY SPACE

These three processes—sharpening of time disparity tuning, elimination of responses to virtual time disparities, and systematic projection of CDs—complete the formation of the azimuthal axis of the auditory space map. The elevational axis of the map is defined by neuronal selectivity for intensity disparity. To produce a two-dimensional map of space, the time and intensity pathways converge on neurons in the ICX. The initial divergence of pathways achieves separate processing and place coding of time and intensity cues, and their subsequent convergence gives rise to a single place-coding scheme for two-dimensional auditory space.

From a Tonotopic to a Nontonotopic Map of Auditory Space

The ICC contains an orderly distribution of neurons representing phase disparities and frequencies; that is, spatial cues and frequencies are mapped in the same array of neurons. Space-specific neurons receive inputs from ICC neurons having the same characteristic delay but different frequency selectivity. Thus we can understand the design of the owl's auditory space map in terms of convergent inputs from the tonotopically organized areas.

Merzenich et al. (1984) argued that because the owl's auditory space map is nontonotopic, it is outside the so-called mainline auditory pathway and is therefore useless in understanding the representation of auditory space in the mammalian brain. They assert further, "Sound localization is frequency specific and requires representation within a projection system resolving spectral components of complex stimuli." They cite as supporting evidence an experiment that demonstrated a cat's inability to localize a tone of a certain frequency after unilateral lesion of the primary auditory cortical area (AI) representing that frequency. This test shows only that the encoding of spatial cues in the primary auditory cortex is frequency specific. The test does not exclude the possible separation of space and frequency in stations beyond the primary auditory cortex. The owl example demonstrates that such a separation is possible. The cat's auditory system also shows a transition from tonotopic to nontonotopic connectivity in the genesis of an auditory space map in the superior colliculus (Middlebrooks and Knudsen, 1984). Therefore, the owl's frequency-nonspecific map of auditory space is not unique.

The absence of tonotopy should be regarded not as an exception but as an indication of specialized functions. A few examples suffice to reveal how the absence of tonotopy may be related to other neuronal characteristics. Like the

cat's superior colliculus, the auditory–visual bimodal map in the barn owl's optic tectum occurs in essentially nontonotopically organized substrates (Knudsen, 1984b). The areas of the mustached bat's auditory cortex containing neurons selective for target range lack tonotopic organization (Suga, this volume). An analogous correlation applies to other neural systems such as the monkey visual cortex in which retinotopic projections are either crude or absent in some of the cortical areas containing neurons selective for complex stimuli (Van Essen, 1985). What the examples above suggest is that some rules govern the separation and combination of place codes for different signals (Konishi, 1986). Thus, the need for either multifrequency convergence or segregation of place codes for other stimulus parameters, or both, is likely to be responsible for the absence of tonotopy.

DISCUSSION AND SYNTHESIS

It is now possible to draw for the owl a coherent picture depicting the parallel and serial processes involved in the analysis of the binaural cues for sound localization from the external ear upstream to the IC. The left–right asymmetries in the external meatus and facial ruff allow time and intensity disparities to vary independently along the azimuthal and elevational axes, respectively. The inner ear performs a frequency analysis in which the amplitude and phase of each frequency channel are determined and encoded. The owl can derive ITDs in a noise from the phase of its spectral components. Binaural phase comparison could allow the owl to discriminate between noises from one source and those from more than one source. This method is very much like the use of binocular disparity sensitivity for the detection of an object against a camouflaged background (Julesz, 1971). Moreover, the encoding of time in phase is less subject to a variation in sound level than to a variation in transient time. Unlike transient disparity, the same phase disparity occurs more than once in most signals.

Phase is transmitted to the brain in the form of phase-locked spikes in the acoustic nerve. The aforementioned cyclical responses of binaural neurons in the time pathway to dichotic stimuli clearly indicate that every cycle is represented, even for high frequencies. A volley mechanism may explain phase coding in high-frequency channels. Amplitude is perhaps encoded by the discharge rate of single neurons. Thus spike discharge of primary auditory fibers contains the codes for both amplitude and phase in each frequency channel. Each CN accepts one code and rejects the other by its own unique synaptic mechanisms. The two codes are thus assigned to separate brain-stem pathways by the distinct projection patterns of each CN. The two codes are obviously not incompatible, because all primary auditory fibers appear to show both phase locking and sensitivity to intensity. Therefore, the reason for the separation may be binaural comparison—the mixing of time and intensity coding parameters of spike discharge is avoided because the absolute time of spike discharge is important for encoding time but presumably not for encoding intensity.

Binaural input to the NL consists of phase-locked spikes from NM nuclei. The NL uses these signals to determine time disparity in each frequency channel. The measurement of time disparities involves axonal delay lines and NL cell

bodies, which act as coincidence detectors. Thus the owl's auditory system performs some sort of cross-correlation on each spectral component of a noise, instead of cross-correlating the unfiltered noise waveform (Yin and Chan, this volume). This procedure is an inevitable consequence of the frequency analysis and coding performed by the inner ear. If cross-correlation of the whole waveform were advantageous, the waveform could, in theory, be represented by recombining the relevant frequency channels. On the other hand, cross-correlation of filtered data has distinct advantages: It improves the signal-to-noise ratio, and it provides bases for nonlinear processing involving different frequency channels, as discussed below.

The NL delay lines are systematically arranged so as to form a map of time disparities in each frequency channel. Each NL neuron represents the phase equivalent of a time disparity as well as a frequency band. Time and frequency are represented not by spike rate or time but by the place of the neuron. The place code is the currency in all further processing of time disparities in stations above the NL. These processes include the enhancement of neuronal selectivity for time disparity and the elimination of response to virtual time disparities. The response to virtual time disparities is due to cross-correlation of sharply filtered data. Enhancement appears to occur within a single-frequency channel, whereas elimination requires convergence of different frequency channels, which takes place in the projection from the ICC to the ICX. The convergence would seem inevitable, if the results of cross-correlation of filtered data are to be of use for time measurement. The results of cross-correlation and subsequent processes are brought together for nonlinear integration, which endows space-specific neurons with their ability to signal their CDs unambiguously. The final stage of encoding the binaural cues for sound localization is the union of the place codes for time and intensity disparities. The union creates a new coding scheme in which each neuron is selective not for time or intensity disparity alone but for a combination of the two. This scheme allows a two-dimensional representation of auditory space.

ACKNOWLEDGMENTS

We thank Drs. E. I. Knudsen and G. A. Manley for critically reading and correcting an early draft of this chapter. This work was supported by National Institutes of Health Grant NS-14617.

REFERENCES

Boord, R. L. (1978) Ascending projections of the primary cochlear nuclei and nucleus laminaris in the pigeon. *J. Comp. Neurol.* 133:523–542.

Carr, C. E., N. Brecha, and M. Konishi (1985) Organization of nucleus laminaris in the barn owl. *Soc. Neurosci. Abstr.* 11:735.

Goldberg, J. M., and P. B. Brown (1969) Response of binaural neurons of dog superior olivary complex to dichotic tonal stimuli: Some physiological mechanisms of sound localization. *J. Neurophysiol.* 32:613–636.

Gross, C. G. (1973) Inferotemporal cortex and vision. *Prog. Physiol. Psychol.* 5:77–115.

Heiligenberg, W., and J. Bastian (1984) The electric sense of weakly electric fish. *Annu. Rev. Physiol.* 46:561–583.

Heiligenberg, W., and G. Rose (1985) Phase and amplitude computations in the midbrain of an electric fish: Intracellular studies of neurons participating in the jamming avoidance response of *Eigenmannia*. *J. Neurosci.* 5:515–531.

Jeffress, L. A. (1948) A place theory of sound localization. *J. Comp. Physiol. Psychol.* 41:35–39.

Julesz, B. (1971) *Foundation of Cyclopean Perception*, Univ. Chicago Press, Chicago.

Knudsen, E. I. (1983) Subdivisions of the inferior colliculus in the barn owl (*Tyto alba*). *J. Comp. Neurol.* 218:174–186.

Knudsen, E. I. (1984a) Synthesis of a neural map of auditory space. In *Dynamic Aspects of Neocortical Function*, G. M. Edelman, W. M. Cowan, and W. E. Gall, eds., pp. 375–396, Wiley, New York.

Knudsen, E. I. (1984b) Auditory properties of spaced-tuned units in owl's tectum. *J. Neurophysiol.* 53:709–723.

Knudsen, E. I., and M. Konishi (1978a) Space and frequency are represented separately in auditory midbrain of the owl. *J. Neurophysiol.* 41:870–884.

Knudsen, E. I., and M. Konishi (1978b) A neural map of auditory space in the owl. *Science* 200:795–793.

Knudsen, E. I., and M. Konishi (1979) Mechanisms of sound localization in the barn owl (*Tyto alba*). *J. Comp. Physiol.* 133:13–21.

Knudsen, E. I., and M. Konishi (1980) Monaural occlusion shifts receptive-field locations of auditory midbrain units in the owl. *J. Neurophysiol.* 44:687–695.

Knudsen, E. I., G. G. Blasdel, and M. Konishi (1979) Sound localization by the barn owl measured with the search coil technique. *J. Comp. Physiol.* 133:1–11.

Konishi, M. (1986) Centrally synthesized maps of sensory space. *Trends Neurosci.* 9:163–168.

Lavine, R. A. (1971) Phase-locking in response of single neurons in cochlear nucleus of the cat to low frequency tonal stimuli. *J. Neurophysiol.* 34:467–483.

Marr, D. (1982) *Vision*, Freeman, San Francisco.

Merzenich, M. M., W. M. Jenkins, and J. C. Middlebrooks (1984) Observations and hypotheses on special organizational features of the central auditory nervous system. In *Dynamic Aspects of Neocortical Function*, G. M. Edelman, W. E. Gall, and W. M. Cowan, eds., pp. 397–427, Wiley, New York.

Middlebrooks, J. C., and E. I. Knudsen (1984) A neural code for auditory space in the cat's superior colliculus. *J. Neurosci.* 4:2621–2634.

Moiseff, A., and M. Konishi (1981) Neuronal and behavioral sensitivity to binaural time difference in the owl. *J. Neurosci.* 1:40–48.

Moiseff, A., and M. Konishi (1983) Binaural characteristics of units in the owl's brainstem auditory pathway: Precursors of restricted spatial receptive fields. *J. Neurosci.* 3:2553–2562.

Molnar, C. D., and R. R. Pfeiffer (1968) Interpretation of spontaneous spike discharge patterns of neurons in the cochlear nucleus. *Proc. IEEE* 56:993–1004.

Parks, T. N., and E. W Rubel (1975) Organization of projections from n. magnocellularis to n. laminaris. *J. Comp. Neurol.* 164:435–448.

Perrett, D. I., E. T. Rolls, and W. Caan (1982) Visual neurons responsive to faces in the monkey temporal cortex. *Exp. Brain Res.* 47:329–342.

Rhode, W. S., D. Oertel, and P. H. Smith (1983) Physiological response properties of cells labeled intracellularly with horseradish peroxidase in cat ventral cochlear nucleus. *J. Comp. Neurol.* 213:448–463.

Rose, J. E., N. B. Gross, C. D. Geisler, and J. E. Hind (1966) Some neural mechanisms in the inferior colliculus of the cat which may be relevant to localization of a sound source. *J. Neurophysiol.* 29:288–314.

Rose, J. E., L. M. Kitzes, M. M. Gibson, and J. E. Hind (1974) Observations on phase-sensitive neurons of anteroventral cochlear nucleus of the cat: Non-linearity of cochlear output. *J. Neurophysiol.* 37:218–253.

Snyder, R. L., and C. E. Schreiner (1984) The auditory neurophonic: Basic properties. *Hear. Res.* 15:261–280.

Sullivan, W. E. (1985) Classification of response patterns in cochlear nucleus of barn owl: Correlation with functional response properties. *J. Neurophysiol.* 53:201–216.

Sullivan, W. E., and M. Konishi (1984) Segregation of stimulus phase and intensity in the cochlear nuclei of the barn owl. *J. Neurosci.* 4:1786–1787.

Takahashi, T. T., and M. Konishi (1986) Selectivity for interaural time difference in the owl's midbrain. *J. Neurosci.* 6:3413–3422.

Takahashi, T. T., and M. Konishi (1988a) Projections of cochlear nuclei and nucleus laminaris to the inferior colliculus of the barn owl. *J. Comp. Neurol.* (in press).

Takahashi, T. T., and M. Konishi (1988b) Projections of nucleus angularis and nucleus laminaris to the lateral lemniscal complex of the barn owl. *J. Comp. Neurol.* (in press).

Takahashi, T. T., A. Moiseff, and M. Konishi (1984) Time and intensity cues are processed independently in the auditory system of the owl. *J. Neurosci.* 4:1781–1786.

Van Essen, D. C. (1985) Functional organization of primate visual cortex. In *Cerebral Cortex*, Vol. 3, A. Peters and E. G. Jones, eds., pp. 259–329, Plenum, New York.

Wagner, H., T. T. Takahashi, and M. Konishi (1987) Representation of interaural time difference in the central nucleus of the barn owl's inferior colliculus. *J. Neurosci.* 7:3105–3116.

Warr, W. B. (1982) Parallel ascending pathways from the cochlear nucleus: Neuroanatomical evidence of functional specialization. In *Contributions to Sensory Physiology*, W. D. Neff, ed., pp. 1–38, Academic, New York.

Weinberger, N. M., L. M. Kitzes, and D. A. Goodman (1970) Some characteristics of the "auditory neurophonic." *Experientia* 26:46–48.

Winter, P., and J. Schwartzkopff (1961) Form und Zellzahl der akustischen Nervenzentren in der Medulla oblongata von Eulen (Striges). *Experientia* 17:515–516.

Yin, T. C. T., and S. Kuwada (1983) Binaural interaction in low-frequency neurons in inferior colliculus of the cat. III. Effects of changing frequency. *J. Neurophysiol.* 50:1020–1042.